

Minor elements in olivine from spinel lherzolite xenoliths: implications for thermobarometry

SUZANNE Y. O'REILLY¹, D. CHEN^{1,2}, W. L. GRIFFIN^{1,3} AND C. G. RYAN³

¹ National Key Centre for Geochemical Evolution and Metallogeny of Continents (GEMOC), School of Earth Sciences, Macquarie University, Sydney, NSW, 2109, Australia

² Department of Earth and Space Sciences, University of Science and Technology of China, Hefei, 230026, P.R. China

³ CSIRO Exploration and Mining, Box 136, North Ryde, NSW 2113, Australia

Abstract

The proton microprobe has been used to determine contents of Ca, Ti, Ni, Mn and Zn in the olivine of 54 spinel lherzolite xenoliths from Australian and Chinese basalts. These data are compared with proton-probe data for Ni, Mn and Zn in the olivine of 180 garnet peridotite xenoliths from African and Siberian kimberlites. Fe, Mn, Ni and Zn contents are well-correlated; because the spinel lherzolite olivines have higher mean Fe contents than garnet peridotite olivines (average $Fo_{89.6}$ vs. Fo_{90-92}) they also have lower Ni and higher Mn contents. Zn and Fe are well-correlated in garnet peridotite olivine, but in spinel peridotites this relationship is perturbed by partitioning of Zn into spinel. None of these elements shows significant correlation with temperature. Consistent differences in trace-element contents of olivines in the two suites is interpreted as reflecting the greater degree of depletion of Archean garnet peridotites as compared to Phanerozoic spinel lherzolites. Ca and Ti contents of spinel-peridotite olivine are well correlated with one another, and with temperature as determined by several types of geothermometer. However, Ca contents are poorly correlated with pressure as determined by the Ca-in-olivine barometer of Köhler and Brey (1990). This reflects the strong T -dependence of this barometer: the uncertainty in pressure (calculated by this method) which is produced by the ± 50 °C uncertainty expected of any geothermometer is ca ± 8 kbar, corresponding to the entire width of the spinel-lherzolite field at 900–1200°C.

KEYWORDS: olivine, minor elements, thermobarometry, mantle, spinel lherzolite, garnet lherzolite.

Introduction

EMPIRICAL geotherms, derived from P - T estimates for garnet+ orthopyroxene+ clinopyroxene \pm olivine xenoliths in basalts and kimberlites, provide an important basis for interpreting the stratigraphy of the upper mantle. However, the required mineral assemblages are rare in xenolith suites from basalts, which typically are dominated by spinel-bearing, rather than garnet-bearing, peridotites. Where a locality has a well-characterised geotherm, T estimates for these lherzolites can be referred to the geotherm to estimate their depth of origin. However, this technique can be used with confidence only in a few regions where suitable garnet-bearing xenoliths occur in sufficient numbers to construct a tightly constrained geotherm (eg. eastern Australia; O'Reilly and Griffin, 1985).

The derivation of a mineralogical geobarometer for the spinel-lherzolite assemblage therefore should be a high priority among empirical and experimental geochemists. Köhler and Brey (1990) have provided experimental calibration of the temperature and pressure effects on the substitution of Ca in olivine coexisting with clinopyroxene, and proposed that their Ca-in-olivine geobarometer can be used (together with appropriate geothermometers) to derive empirical geotherms for spinel lherzolite assemblages. One limitation on the use of this geobarometer is the difficulty of achieving high-precision analyses of Ca at ppm levels. However, this problem can be solved by the use of the proton microprobe, which gives rapid analysis of Ca with precision (1σ) of ca. 2–3% at the 200 ppm level. In this paper we report the proton-microprobe analysis of Ca in olivine from 54 spinel lherzolite xenoliths,

and use these data to test the application of the Ca-olivine geobarometer. The samples come from four localities in eastern China, and four areas in eastern Australia. Pressures derived for the Australian samples can be compared with those expected by reference to the well-constrained xenolith geotherm of O'Reilly and Griffin (1985).

The proton microprobe also provides analyses of Ti, Mn, Ni and Zn in olivine. We use these data to constrain interelement relationships in olivine from spinel lherzolites over the depth range 25–55 km, and to compare with similar data for 180 garnet peridotite xenoliths from kimberlites, mainly in South Africa and Siberia. These data help to define the abundances of some important minor elements in the subcontinental lithospheric mantle, data which are important for large-scale geochemical modelling.

Methods

To avoid grain-boundary fluorescence effects, samples were analysed as grain mounts. Five whole olivine grains were picked from each rock, following delicate disaggregation of a small volume. Most grains are 0.5–2 mm in diameter; some are larger. The grains were mounted in epoxy blocks and polished before being analysed for major elements by electron microprobe (EMP) in the GEMOC National Key Centre in the School of Earth Sciences, Macquarie University (see Chen *et al.* (1991) for details). Each grain was analysed at two spots, to check for homogeneity and samples showing heterogeneity either within or between grains were discarded.

Trace element analyses were carried out by PIXE (Particle Induced X-ray Emission), using the HIAF proton microprobe at CSIRO Exploration and Mining, North Ryde. The instrument is based on a tandem

electrostatic accelerator, which delivers a beam of 3 MeV protons, focussed to a spot 20–30 micrometres in diameter on the sample; the analysed volume extends to depths of *ca.* 35 μm . Generated X-rays are collected by a Si(Li) energy-dispersive detector, giving a spectrum that is reduced as described by Ryan *et al.* (1990). Thin foils are placed between the sample and the detector to attenuate major-element lines, and thus to allow use of higher beam currents and shorter analysis times. In the present case, the problem is to attenuate the Fe lines, but still to allow analysis of the lighter elements, specifically Ca. This was achieved by use of a Mylar-backed Cr foil (thickness 6 mg/cm²); the absorption edge of the Cr strongly attenuates the Fe peaks, while allowing the X-rays of Ca, Ti etc. to be seen. The combined Cr+Mylar filter, together with the Be window on the detector itself, attenuates the lines from Si and Mg. Fluorescence of the Cr filter by Fe X-rays produces Si escape peaks of Cr, which partially overlap the peaks of Ca and Ti. This interference was corrected by measurement of the peak areas as a function of Fe content to provide an empirical correction, which typically was at the level of 50–80 ppm on Ca and 5–10 ppm on Ti. In the discussion below, the present data on spinel lherzolites are compared with a larger database of analyses of olivine in garnet peridotite xenoliths from kimberlites. These all have been analysed using a 200 μm Al filter, rather than the Cr filter used for the spinel lherzolites, so that data are available only for Mn, Ni and Zn. To ensure comparability, several samples were analysed by both techniques; this revealed small but consistent discrepancies in Mn and Ni (*ca.* 10%), which are ascribed to uncorrected absorption effects in the Cr-filter runs. The Cr-filter data for Mn and Ni therefore have been corrected to make the two data sets compatible. No corrections were required for Zn data.

TABLE 1. Analyses of standard olivines

Element	SC-1 Standard Olivine			N-1 Standard Olivine		
	PMP	Nominal	EMP	PMP	Nominal	EMP/SIMS
Ca	518 ± 14	524 ± 4 (ID)	523 ± 10	25 ± 7	19.6 ± 3 (ID)	19.8 ± 1.1 (SIMS)
Ti	28 ± 2	na			8 ± 2	na
Mn	1230 ± 100	1065 ± 32 (INAA)			870 ± 50	734 ± 2 (INAA)
Ni	2710 ± 200	2950 ± 150 (INAA)	2990	3040 ± 200	3130 ± 100 (INAA)	2750 (EMP)
Zn	56 ± 2	60 ± 9 (INAA)		36 ± 2	38 ± 3 (INAA)	

PMP = Proton Microprobe

INAA = Instrumental Neutron Activation analysis

EMP = Electron Microprobe

ID = Isotope Dilution

SIMS = Secondary Ion Mass Spectrometry

Each grain was analysed in one spot in the core, using an accumulated live charge of 1 μC ; typical analysis times were 5–6 minutes. The individual spectra for the grains in each sample were then digitally summed (omitting any clear outliers) to produce a composite spectrum with higher statistics. The standard deviation for the Ca analyses (calculated from counting statistics) of the single spectra typically was $\pm 8\%$ at 200 ppm (200 ± 15 ppm) and $\pm 3\%$ at 700 ppm (700 ± 20 ppm). For the summed spectra, the corresponding values are $\pm 5\%$ and $\pm 2\%$. This corresponds to a Minimum Detection Limit (calculated at the 99% confidence level) of ca. 12 ppm Ca. The data from the summed spectra are presented in Tables 1 and 2.

The proton-microprobe technique used here is independent of standards (Ryan *et al.*, 1990). Accuracy was assessed by analysis of two standard olivines (Köhler and Brey, 1990) kindly supplied by A.L. Jaques. The data for these two standards show excellent agreement with the nominal values (Table 1).

Xenolith samples

The samples used here were collected from four widely separated areas: western Victoria, southern Queensland and northern Queensland in Australia, and the Jiashan-Luhe volcanic field northwest of Nanjing in eastern China. Centres sampled in western Victoria include the Wiridgil Hills, The Anakies, the maars at lakes Bullenmerri and Gnotuk, and Mount Leura (Griffin *et al.*, 1984; Chen *et al.*, 1991). The southern Queensland samples come from Gowrie Mountain (Chen *et al.*, in prep.) near Toowoomba. The northern Queensland samples are from several craters in the Atherton, Chudleigh and McBride provinces (Stephenson, 1989). In the Jiashan-Luhe field, samples come from four cinder cones: Nushan in Jiashan County and Panshishan, Fashan and Pinshanlinchang in Luhe County (eg. Dostal *et al.*, 1988).

All of the above samples contain the spinel-lherzolite assemblage (ol+cpx+opx+spinel), and thus will be referred to as lherzolites, although some contain less than 5% cpx and thus would be classified as harzburgites by most petrographic classification schemes. Most samples range from 5–25 cm in diameter, and were chosen for their lack of alteration or penetration by the host basalt, and relatively coarse grain size. Several of the Western Victoria samples have been described in detail by O'Reilly and Griffin (1988) and Griffin *et al.* (1988); they show extensive cryptic and modal metasomatism (addition of amphibole \pm apatite), and were included here specifically to examine the effects of these processes on element distribution and geothermo-

barometry. Two of the Nushan samples also contain amphibole, interpreted as the result of metasomatism. All of these xenoliths have been brought to the surface by eruption of primitive alkali basalts, and are interpreted as samples of Phanerozoic subcontinental lithosphere (O'Reilly and Griffin, 1988; Griffin *et al.*, 1996; Xu *et al.*, 1996), on the basis of their geological setting.

The data on olivines from garnet peridotites, used for comparison here, were collected during the course of other studies from a wide range of garnet peridotite xenoliths, including lherzolites, harzburgites and dunites, some of which show cryptic or modal metasomatism. The sample includes both low-*T* xenoliths with granular microstructures and high-*T* xenoliths with strongly foliated microstructures. The xenoliths used here are from kimberlites in southern Africa and Siberia, and thus represent samples of the mantle beneath areas with Archaean cratonic crust.

Results

Analytical data for olivine grains from 54 xenoliths are presented in Table 2. The average values and standard deviations for the trace elements are derived from the summed PIXE spectra.

(1) *Iron.* FeO contents vary mainly from 8.6 to 11.3% (with three outliers at 13–14%), corresponding to a range in Fo content from 86–91% (mean 89.6%). This covers most of the range reported in typical spinel lherzolite xenoliths in alkali basalts worldwide. All but one of the samples are within the range of $\text{Fo}_{90 \pm 3}$ that Köhler and Brey (1990) accept as the range of application for their Ca barometer. The average FeO content of olivine in 54 spinel lherzolites analysed here is $10.2 \pm 0.8\%$ (1 standard deviation); the corresponding value for olivine in 180 garnet peridotites from South African and Siberian kimberlites in our database is $7.7 \pm 1.1\%$.

(2) *Calcium.* Ca varies from 42–1200 ppm; most values are in the range 200–600 ppm (mean 380 ± 210 ; median ≈ 360 ppm), and there is no clear relationship of Ca contents either to locality or to the presence or absence of amphibole in the rock. A plot of Ca vs. FeO (Fig. 1) shows no overall correlation.

(3) *Titanium.* Ti ranges from <5 –124 ppm, with most values between 10–30 ppm (mean 21 ± 17 ; median ≈ 18 ppm). Two high-Ca outliers (FS3 and FS5) both show very homogeneous Ti contents (high and low, respectively). There is a good correlation between Ca and Ti (Fig. 2). There is no correlation between Ti contents and locality, or between Ti content and the presence of amphibole. The two international standards (Table 1) lie on the same trend. This may indicate that Ti substitution is partly controlled by the distortion of the olivine lattice caused by the substitution of Ca for Fe.

TABLE 2. Analytical data for olivine and *P-T* estimates

	FeO, %	Ca	Ti	Mn	Ni	Zn	T,Wells °C	P,KB90 kB	T,S&S °C	P,KB90 kB	T,BK90 °C	P,KB90 kB	metasom. kB
W. Victoria													
<i>Wiridgil Hills</i>													
WH2	9.13	377	7	1000	2750	52	910	7.4	884	4.3	899	6	
WH6	10.3	394	19	1090	2990	63	967	10.1	936	6.5	1003	11	
WH8	8.75	277	8	950	2980	54	909	15.3	823	4.4	900	14.1	
<i>The Anakies</i>													
An20	10.9	306	18	1163	2710	48	925	13.6	973	19.5	946	16.2	
An21	10.2	264	18	1095	2550	40	916	17.2	960	22.2	919	17.6	
An22	10.7	195	7	1170	2840	54	876	19.9	872	19.3	874	19.5	
An23	11.2	211	14	1030	3245	46	883	19.7	872	18.3	866	17.4	
<i>Bullenmerri area</i>													
WGBM1	10.8	261	15	1140	2500	51	884	9.2	961	18.9	834	3	A
WGBM2	10.8	209	18	1040	2610	48	869	13.9	1130	47.6	830	8.8	A
WGBM5	9.78	445	44	1220	2820	56	990	7.2	1054	15.5	1036	12.4	
WGBM15	11.2	250	12	1170	2750	74	927	15.6	1000	15	955	19.1	A
SGN1	8.62	196	10	960	2890	55	846	13	890	18.9	814	8.8	AAp
BM901	13	242	12	1380	2400	84	916	13.1	840	3.6	928	14.7	AAp
LE16B	8.75	470	23	980	2800	51	957	5	1030	12.6	930	1.8	
9708	9.65	172	10	1060	2740	42	871	20.1	867	19.5	841	16	A
9894	11.3	468	47	1180	2540	52	993	3.6	1050	14	1036	10.9	
<i>S. Queensland</i>													
GM1	10.0	146	17	1060	2750	33	929	34.7	1008	35.4	932	35.1	
GM2	10.0	475	16	1080	2700	51	929	2.4	1027	12.7	905	-0.4	
GM5	10.4	106	7	1100	2750	27	776	33.7	1033	49.5	703	11.7	
GM8	10.4	516	18	1130	2790	49	959	2.2	983	4.8	987	5.3	
GM10	14.0	425	22	1060	1970	79	955	7.5	1015	12.2	976	9.9	
GM12	10.4	455	20	1120	2690	45	893	-0.2	1021	13	879	-1.9	
GM13	10.4	494	22	1130	2600	56	949	3.1	1009	8.1	971	5.6	
GM14	10.0	500	19	1090	2680	43	928	0.2	971	5	948	2.5	
GM15	10.0	558	22	1090	2660	52	1045	9.7	991	1.8	1110	20.7	
GM16	10.0	516	22	1090	2650	52	939	0.5	972	4.2	962	3.1	
GM17	10.3	516	21	1120	2720	49	942	1	993	6.7	980	5.3	
GM18	10.0	246	<4.6	1070	2740	33	933	20.6	975	26.1	961	24.3	
GM19	10.0	523	21	1090	2745	48	869	-6.3	959	4	806	-13.5	
HQ1	11.1	157	16	1150	2740	38	956	35.9	936	33.1	963	36.9	
<i>N. Queensland</i>													
N5-10	10.2	251	17	1090	2690	39	867	13.6	893	17.1	808	4.8	
N6-5	10.2	165	9	1080	2720	32	812	17.1	860	23.9	709	2.5	
N8-10	10.4	278	9	1150	2620	44							
N19-3	10.7	386	26	1120	2520	45	973	12.7	994	15.2	980	13.5	
N26	10.2	285	22	1080	2760	40							
E. China													
<i>Panshishan</i>													
PS2	10.2	346	26	1100	2630	46	947	12.8	1025	18.9	941	12.1	
PSS2	9.52	457	26	910	2770	50	930	2.4	1037	14.2	938	3.3	
PSS3	10.3	491	27	980	2770	54	975	4.7	1055	15.1	1004	6.4	
PSS6	10.9	308	19	1060	3270	60	915	11.6	935	14.1	921	12.3	
PSS7	10.9	725	37	980	2500	72	1089	9	1094	2.3	1162	20.9	
<i>Nushan</i>													
Nush1	10.9	208	5	1150	2510	76	829	9.2	947	24.7	803	5.8	A
Nush4	9.87	197	45	1030	2730	50	849	15.5	977	32.8	802	9.1	A
Nush5	10.2	466	23	1000	2590	54	1047	13.3	1070	17.1	1115	24.9	
Nush6	10.4	609	29	1020	2500	56	1056	6.5	1103	17	1090	14.9	
Nush7	10.4	611	30	1010	2500	56	1051	8.5	1111	18.6	1096	16	

TABLE 2 (contd)

	FeO, %	Ca	Ti	Mn	Ni	Zn	T,Wells °C	P,KB90 kB	T,S&S °C	P,KB90 kB	T,BK90 °C	P,KB90 kB	metasom. kB
<i>Fangshan</i>													
FS1	10.6	386	25	1100	2690	59	894	3.2	1012	14.1	849	-2.1	
FS2	10.0	613	31	1080	2670	52	992	-0.2	1081	14	1016	3.2	
FS3	13.0	1198	124	1180	2520	97	1150	5.1	1192	11.5	1193	11.6	
FS4	9.78	183	10	1090	2730	42	831	15.6	924	28.3	772	7.4	
FS5	9.39	1080	16	1040	2710	53	1117	6.3	1139	9.8	1134	9.1	
<i>Pinshanlinchang</i>													
PL2	9.78	350	20	1060	2660	47	989	19.7	979	18.4	987	19.4	
PL3	8.49	42	14	940	2650	30	836	57.9	871	64	724	38.3	
PL4	10.0	315	22	1080	2600	43	952	16.7	964	18.3	968	18.8	

A indicates amphibole present
 AAp indicates amphibole and apatite are present

(4) *Manganese*. Mn ranges from 910–1380 ppm, with most values from 1000–1200 ppm. Mn is well-correlated with Fe (Fig. 3), and shows no relation either to locality or to the presence of amphibole. Figure 3 also shows data for olivine in 180 garnet peridotite xenoliths from African and Siberian kimberlites; these cover a wider range of both Fe and Mn, and show a similar but less well-defined correlation between the two elements. The average content of Mn in the olivine of spinel lherzolite

xenoliths is 1080 ± 80 ppm (1 standard deviation). The corresponding value for olivine in garnet peridotite xenoliths from kimberlites is 795 ± 190 ppm. The mean Fe/Mn for all olivines is about 7.

(5) *Nickel*. Ni ranges from 1970–3270 ppm. There is a weak negative correlation between Ni and FeO in the spinel-lherzolite olivines (Fig. 4a), and a better-defined correlation within the garnet peridotite suite. Ni is weakly correlated with Mn, reflecting their mutual dependence on Fe contents (Fig. 4b). The spinel lherzolite olivines contain somewhat less Ni than the olivines of garnet peridotites, corresponding to the difference in mean FeO between these two populations. The average Ni content of the spinel-

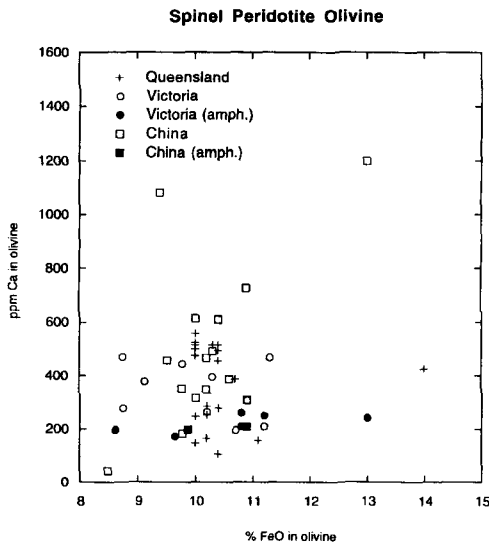


FIG. 1. Ca vs. FeO in olivines from spinel peridotite xenoliths; data from Table 2.

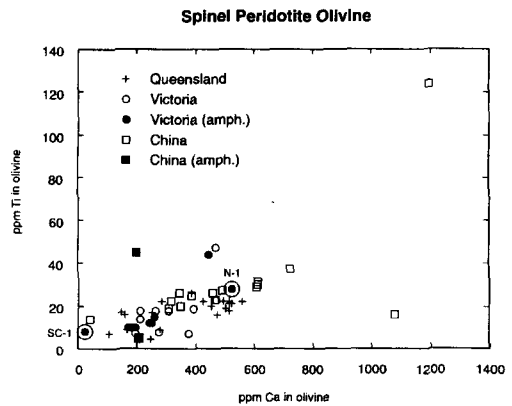


FIG. 2. Ca vs. Ti in olivines from spinel peridotite xenoliths; data from Table 2. Standard olivines (Table 1) circled.

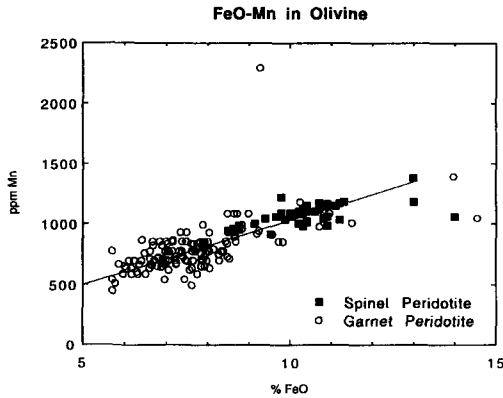


FIG. 3. Mn-FeO relationship in olivines from spinel peridotite xenoliths (Table 2) and garnet peridotites (Griffin and Ryan, unpubl. data). Line is given by: $Mn(\text{ppm}) = 105 * \text{FeO}(\%) - 25$.

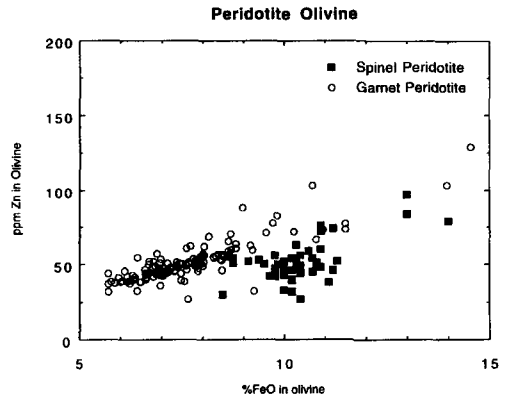


FIG. 5. Zn-FeO relationship in olivines from spinel peridotite xenoliths (Table 2) and garnet peridotites (Griffin and Ryan, unpubl. data).

Discussion

Temperature effects

lherzolite olivines is 2690 ± 190 ppm; the average Ni content of garnet-lherzolite olivine ($n = 180$) is 2930 ± 480 ppm.

(7) *Zinc*. Zn ranges from 33–97 ppm, with most values between 40 and 70 ppm. Zn is not well-correlated with FeO in the spinel-lherzolite olivines (Fig. 5), and there is no obvious relation to locality or to metasomatism (as defined by presence of amphibole \pm apatite). In contrast to the spinel lherzolites, the data from South African and Siberian garnet peridotites show a good overall correlation between Fe and Zn, with higher Zn contents at equivalent Fe levels. The average Zn content of mantle olivine is 55 ± 20 ppm ($n = 240$).

Temperatures have been calculated for the spinel lherzolite xenoliths using the two-pyroxene thermometer of Wells (1977), the Ca-in-orthopyroxene thermometer of Köhler and Brey (1990) and the olivine-orthopyroxene-spinel thermometer of Sachtleben and Seck (1981; Table 2).

With one exception, FeO content of olivine from amphibole-bearing rocks broadly increases with increasing T (Fig. 6), whereas no clear trend is visible for olivine from amphibole-free rocks. A general decrease in FeO with increasing temperature is expected, because the associated pyroxenes and

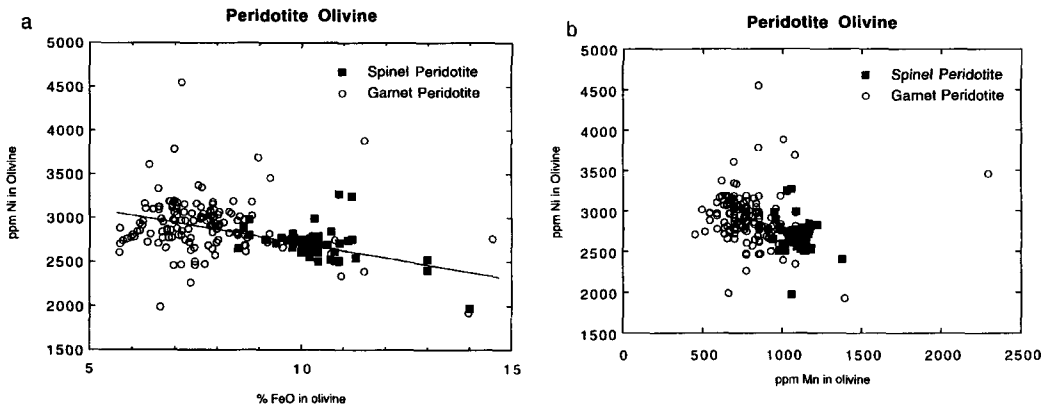


FIG. 4. Ni in olivines from spinel peridotite xenoliths (Table 2) and garnet peridotites (Griffin and Ryan, unpubl. data). (a) Ni vs. FeO; (b) Ni vs. Mn. Line is given by: $Ni(\text{ppm}) = 3500 - 80 * \text{FeO}(\%)$

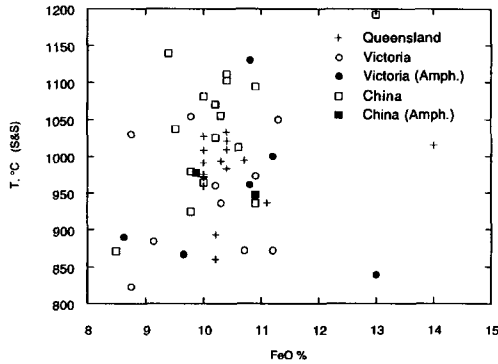


FIG. 6. Variation of Fe with temperature in olivines from spinel peridotites, using geothermometer of Sachtleben and Seck (1981); data from Table 2.

spinel become more Mg-rich with increasing T (eg. O'Neill and Wall 1987). However, the Fo content of the olivine also will reflect bulk composition, whether these differences are caused by primary processes, or by metasomatism, and the general lack of a correlation in Fig. 6 suggests that bulk-composition effects are most important.

Ca contents show an excellent overall correlation with T (Fig. 7); this reflects the temperature-dependent partitioning of Ca between olivine and clinopyroxene, which has been studied in several experiments (Köhler and Brey (1990), and references therein). In detail this correlation shows two segments with different slope, above and below approximately 1000 °C, though the higher- T segment is not well-defined. This break in slope is independent of the thermometer used. Nixon (1987) presented data on Ca in olivine from garnet peridotite xenoliths from East Griqualand; olivine from low- T xenoliths (800–1000 °C) contained 150–400 ppm Ca, and olivine from high- T xenoliths (1100–1300 °C) contained an average 800–900 ppm Ca. These values lie within the band shown in Fig. 7, and suggest that the break in slope may be independent of the tectonic setting (and hence geotherm).

A similar change in slope was observed in experimental studies of Ca solubility in olivine by Köhler and Brey (1990); they suggested that an apparent change in the solubility above 1100°C may be related to order-disorder phenomena in the olivine lattice. This interpretation is supported by single-crystal *in situ* neutron diffraction experiments at high temperature (Artioli *et al.*, 1995) which show that Fe^{2+} partitioning between the octahedral sites in olivine is reversed above 900°C with Fe^{2+} preferentially ordering into the $M2$ site at high temperatures, contrary to previous assumptions used for thermodynamic models. Alternatively, the break in slope

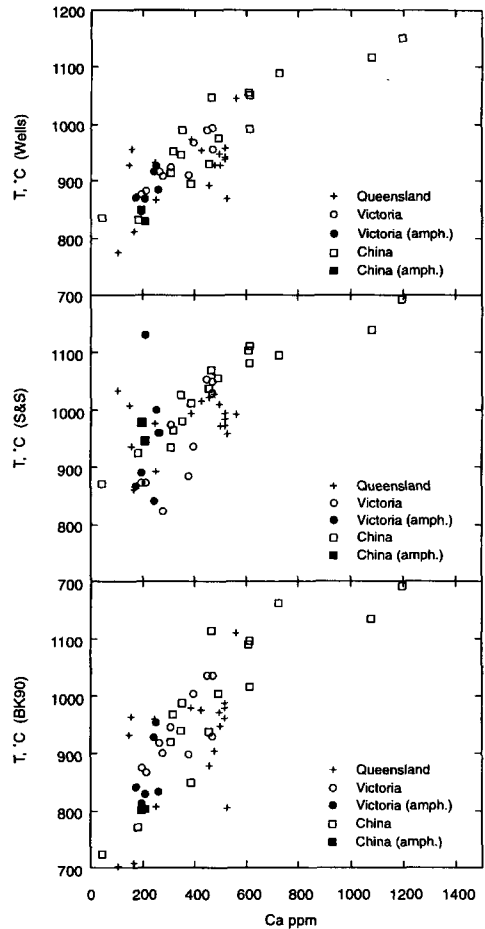


FIG. 7. Variation of Ca with temperature in olivines from spinel peridotites, using different geothermometers discussed in text; data from Table 2.

may reflect changes in Ca partitioning between olivine and clinopyroxene, due to increasing substitution of Tschermak's molecule in the clinopyroxene with increasing T .

The standard olivine N-1 comes from the well-studied peridotite (garnet lherzolite to spinel-amphibole lherzolite) body at Åheim in Almklovdalen, Norway, and samples from this body give two-pyroxene temperatures of 700–750 °C (Griffin, 1987). Olivine N-1 thus would plot near the low- T extension of the Ca- T trend (Fig. 7), and this suggests that little Ca substitutes into olivine below this T .

Titanium contents also are well-correlated with T (Fig. 8), as would be expected from the good correlation between Ca and Ti (Fig. 2). A break in

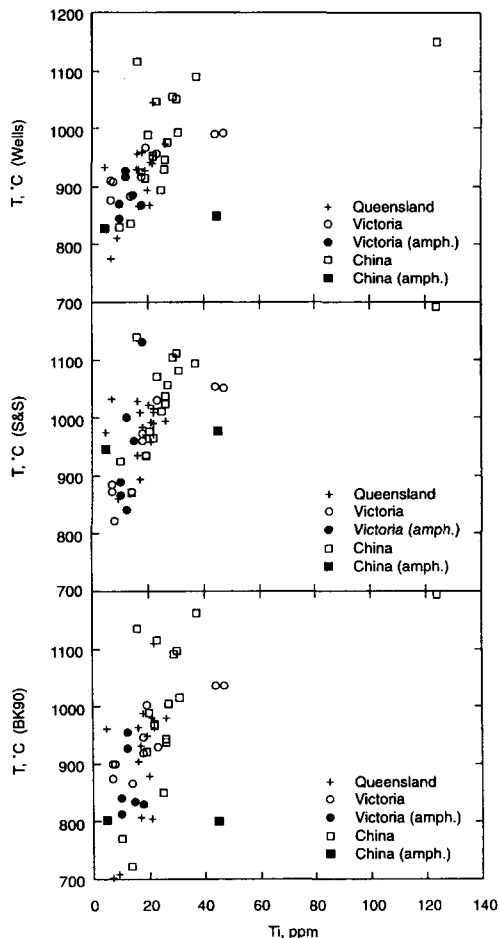


FIG. 8. Variation of Ti with temperature in olivines from spinel peridotites, using different geothermometers discussed in text; data from Table 2.

slope above 1000°C, like that seen in the Ca– T plots, may exist but it is not well-defined by the other data. Unlike Ca, Ti is not directly buffered by any Ti-rich phase in the lherzolite assemblage, and the control behind the correlation of Ti with T is not obvious. One possibility is the effect of the temperature and pressure dependence of the coupled substitution between Al and Ti in clinopyroxene. Wass (1973, 1979) and Yagi and Onuma (1967) showed that Ti and Al^{iv} are partitioned more strongly into the clinopyroxene structure with decreasing pressure (P), whereas the Ti-free Ca-Tschermak's molecule is favoured as P increases: this results in increasing the Al^{vi}/Al^{iv} ratio and decreasing Ti content with increasing P (Aoki and Shiba, 1973). On the high geotherms represented by the samples in this study

(see below), P increases rapidly with increasing T . The increase in Ti with T , therefore, may reflect the rejection of Ti by the pyroxene, and a consequent change in the buffer system (eg. increase in the partition coefficient for Ti between olivine and clinopyroxene).

Mn, Zn and Ni contents appear to be controlled primarily by Fe content, which appears to be only weakly dependent on T (Fig. 6). As a result, the Mn, Zn and Ni contents show no clear dependence on T .

The data for Ca and Ti underscore the usefulness of trace elements in minerals as indicators of environmental conditions, especially temperature. The Ca contents of olivines in the present datasets vary by nearly two orders of magnitude over a T range of 400°C, compared with a factor of two for Fe.

Metasomatic effects

The Ca– T plot (Fig. 7) shows that most of the variation in Ca contents of olivine can be explained in terms of the temperature effect. The correlation between Ca and Ti (Fig. 2) shows that the same is true of Ti. If these elements have been added to the amphibole-bearing samples by metasomatism, then the levels of Ca and Ti in the olivine apparently have been buffered by partitioning with clinopyroxene (and/or amphibole).

The good correlations between higher average Fe, Mn and Zn contents in the amphibole-bearing samples strongly indicate that these elements were introduced together by metasomatism. The poor correlation between FeO and T may indicate that metasomatism occurred (or the assemblages re-equilibrated) over a wide T range.

Spinel vs. garnet peridotites

Comparison of the present data on spinel lherzolites with those from a larger database of garnet peridotite xenoliths reveals some significant differences. Average Fe is higher in the olivines of the spinel peridotites, and this is accompanied by higher Mn and lower Ni, as these elements closely follow Fe. There is no obvious mineralogical reason for these differences; although garnet may have a higher Fe/Mg than spinel, each makes up a small part of the respective assemblages (typically $\ll 5\%$). Similarly, there is no consistent temperature difference between the rocks in the two datasets. It seems clear that these differences in olivine composition reflect real bulk composition differences between the two sets of rocks, rather than being directly connected with the difference in their metamorphic facies.

Boyd (1989) has demonstrated that garnet peridotite xenoliths in kimberlites that penetrate regions of Archaean crust (and thus sample presumed

Archaean lithosphere) are typically strongly depleted (as reflected in high-Mg olivine and low contents of clinopyroxene and garnet) and relatively high in Mg/Si compared to oceanic peridotites and other rocks that might be residual from partial melting at relatively shallow depth. Boyd (1996) has expanded this work to show that many suites of xenoliths from Phanerozoic areas have compositions similar to the oceanic peridotites, and distinct from Archaean garnet peridotites. Xu *et al.* (1996) have confirmed this for the Nushan xenoliths and J. McCarron (pers. comm., 1996) has found similar relationships in the xenoliths from eastern Australia studied here. We therefore suggest that the overall differences in olivine composition between the garnet peridotites and spinel lherzolites presented here reflect fundamental differences in fertility between Archaean and Phanerozoic lithospheric peridotites.

The differences in Fe/Zn between the olivines of the two rock types, however, may reflect their mineralogical differences. Mantle spinels can take up several hundred ppm of Zn, while most mantle silicates have similarly low Zn contents (O'Reilly *et al.*, 1991; O'Reilly and Griffin, 1995; Griffin and Ryan, unpubl. database). The olivines of the spinel peridotites have a mean Zn content of approximately 50 ppm, compared with *ca.* 75 ppm in garnet-peridotite olivines of similar Fe content. The presence of 2–5% spinel with 500–1000 ppm Zn would be enough to account for the lower Zn content of the spinel-peridotite olivines.

Pressure effects

The Ca-in-olivine barometer. Köhler and Brey (1990) reported an experimental study of Ca solubility in olivine that produced the first systematic reversed results showing a pressure dependence of Ca partitioning between clinopyroxene and olivine. Previous theoretical and experimental studies (eg. Finnerty and Boyd, 1978; Adams and Bishop, 1982, 1986; Finnerty, 1989) did not give useful results for natural mineral assemblages (see discussion by Köhler and Brey, 1990). Köhler and Brey overcame the shortcomings of previous studies by using natural rock compositions and by analysing the run products as grain mounts to avoid phase-boundary fluorescence effects on the analysis of Ca. By careful analysis, they produced EMP data for Ca with a precision of 3% relative at the 500 ppm Ca level, and 7% relative at the 200 ppm level.

The results reported by Köhler and Brey show consistent *P* dependence of Ca partitioning in the *P*–*T* range relevant to garnet peridotite xenoliths from kimberlites, but the results from the spinel-lherzolite stability field are less clearcut. As shown in Fig. 9, there are only five runs in or near this field,

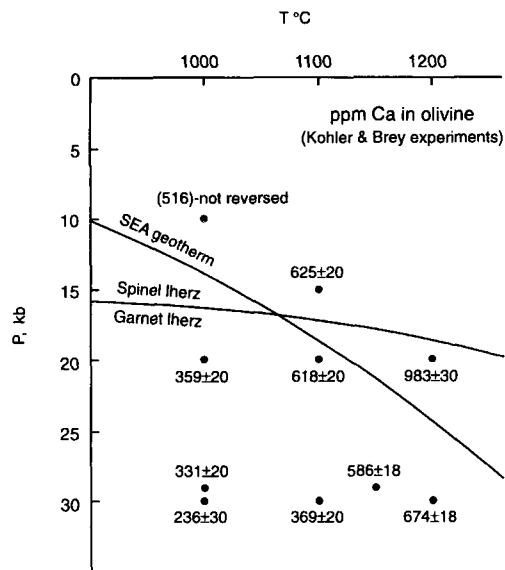


Fig. 9. Experimental data on Ca concentration of olivine coexisting with clinopyroxene, in the *P*–*T* range represented by the spinel-lherzolite assemblage (Köhler and Brey, 1990). The southeastern Australia (SEA) xenolith-based geotherm of O'Reilly and Griffin (1985) is shown for reference, as well as the stability field of the spinel-lherzolite assemblage (Herzberg, 1978), for compositions appropriate to these peridotite xenoliths (O'Neill, 1981).

and the results show a strong dependence of Ca on *T*, but no clear *P* dependence. The 1000 °C, 10 kbar run was not completely reversed, and the reported Ca content represents "the midpoint between minimum and maximum Ca content". Therefore, no *P* dependence of Ca in olivine is defined in the spinel lherzolite *P*–*T* range, and the application of the Ca barometer to spinel lherzolites depends on the extrapolation of data from higher *P* and/or *T*. On the other hand, the strong *T* dependence of the Ca partitioning allows the use of the "barometer" as a thermometer, as discussed by Köhler and Brey (1990).

Application to spinel lherzolites. An empirical geotherm has been constructed for the Bullenmerri-Gnotuk locality in Western Victoria (Griffin *et al.*, 1984; O'Reilly and Griffin, 1985) using garnet websterite xenoliths entrained from a wide depth range, covering most of the spinel lherzolite stability field. A careful examination of geothermobarometers was carried out during this work, to choose those that give *P*–*T* estimates consistent with experimental data on the transition between spinel and garnet

websterite assemblages. Composite garnet websterite–spinel lherzolite xenoliths were then used to test geothermometers for the spinel lherzolite assemblage. Several were found which give temperatures for the spinel lherzolites that are concordant with the P – T estimates from the coexisting garnet websterites. Our thermometer of choice for the lherzolites is that of Sachtleben and Seck (1981), based on the distribution of Fe/Mg, Al and Cr between olivine, orthopyroxene and spinel. This thermometer (and its revision by Witt-Eickschen and Seck (1990)) also avoids the problems noted by Köhler and Brey, related to reequilibration between two pyroxenes during cooling of the mantle. We have previously noted (Chen *et al.*, 1991) that the Brey and Köhler (1990) thermometer, based on the exchange of the enstatite component between clinopyroxene and orthopyroxene, gives temperatures that appear to be too high, considering the constraints mentioned above.

A very similar geotherm has been derived by Xu *et al.* (1996) for the Nushan locality, using garnet websterite and garnet peridotite xenoliths; these authors also carried out a re-evaluation of the geothermobarometry and concluded that the P – T protocol for garnet websterites adopted by Griffin *et al.* (1984) is robust and preferable in many respects to several more recent geothermometers. Xu *et al.* (1996) also concluded that the Köhler and Brey (1990) Ca-in-orthopyroxene thermometer gives temperatures for both websterites and peridotites that are comparable to those of the Sachtleben and Seck (1981) thermometer, in magnesian assemblages.

An important feature of the Nushan and SEA geotherms is the elevated temperature at relatively shallow depths and the strongly concave shape of the geotherm; both imply advective heat transfer and high surface heat flows, consistent with basaltic volcanism. The shape and position of these geotherms, and the depths to the crust–mantle boundary implied by them, have been shown to be consistent with geophysical data from the specific regions of eastern Australia and eastern China to which they refer (O'Reilly and Griffin, 1985; Xu *et al.*, 1996).

Table 2 shows P estimates, derived from the Ca-in-olivine barometer of Köhler and Brey (1990) and three different geothermometers. The P – T estimates for the Victorian and Nushan spinel lherzolites would be expected to plot near the empirical xenolith-derived geotherm. While there is a general correlation between P and T within these suites (Fig. 10), the data cannot be said to follow the geotherm derived from the coexisting garnet websterites and garnet peridotites, regardless of the thermometer used. Although some points fall near the previously derived geotherm, others scatter away from it by as

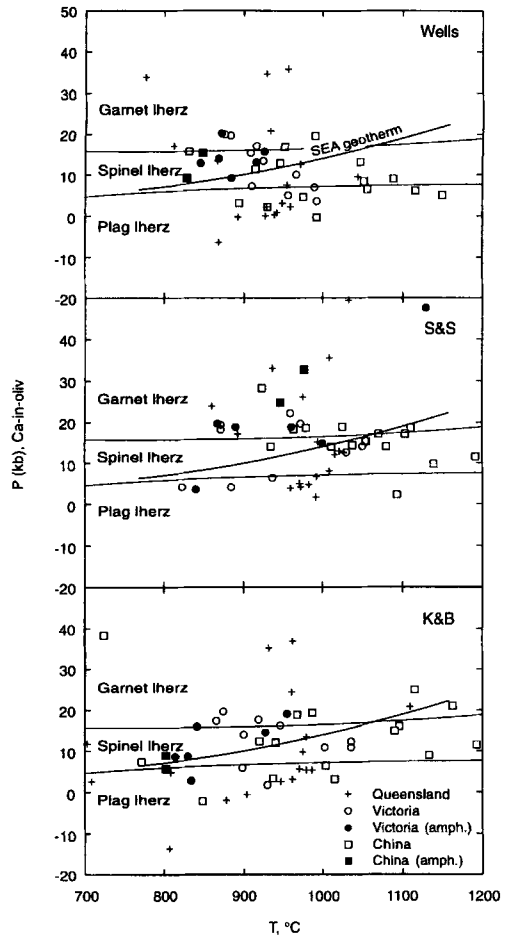


FIG. 10. P – T estimates for spinel lherzolites from Victoria and China, derived by application of the Köhler and Brey (1990) two-pyroxene geothermometer and Ca-in-olivine geobarometer. Data from Table 2. The southeastern Australia (SEA) geotherm and the stability field of the spinel-lherzolite assemblage are the same as for Fig. 9. Data from the Victoria and China localities, at least, would be expected to plot near (± 2 kbar) the SEA geotherm.

much as 10 kbar at any T . A number of points give low pressures that would lie in the olivine+plagioclase stability field, and several others give high pressures that would require the presence of garnet in these relatively fertile rocks. There is even greater scatter for some of the other suites, in which many samples give very low to negative pressures, or extremely high pressures, and in which the P – T correlations may be negative. We conclude that the

TABLE 3. Error analysis of the Ca-in-olivine geobarometer

Test 1. <i>T</i> variation with Ca content					
Assumed starting compositions: Cpx 19.09% CaO, Olivine 0.06% CaO					
CaO in olivine	D	T, °C	P, kbar	P-P1 (kbar)	P-P1 (%)
0.060%	0.00217	1036	13.8		
0.066%	0.00239	1027	9.9	-3.9	-28
0.054%	0.00196	1047	18.0	4.2	30

Test 2. Effect of <i>T</i> uncertainty on <i>P</i>		
Assumed starting compositions as above		
CaO in olivine	Assumed T (°C)	Calc P (kbar)
0.060%	1100	24.8
	1200	42.2
0.066%	1100	22.5
	1200	39.6
0.054%	1100	27.3
	1200	44.8

pressure estimates for spinel lherzolite xenoliths, derived from the Ca-in-olivine geobarometer, cannot be used to define the geothermal gradient in the lithosphere.

Error analysis. A simple error analysis illustrates the difficulty of using the Ca content of olivine as a barometer, even if the extrapolation of the high-*P* experimental data into the spinel-lherzolite *P-T* field is accepted as valid. There are two significant sources of error: uncertainty in the analysis of Ca at low levels in olivine, and the problems involved in the choice and application of a geothermometer. The effects of these uncertainties are shown in Table 3. Even with the use of the proton microprobe, the analytical uncertainty (1σ) on a Ca analysis at the 300 ppm level is *ca.* 2–3%. For careful EMP analysis, $\pm 10\%$ is a reasonable estimate for the uncertainty at these natural levels. In the example shown in Table 3, with an olivine with 600 ppm CaO (425 ppm Ca) and a *T* of 1300 K, an analytical uncertainty of $\pm 10\%$ gives an uncertainty in calculated *P* of *ca.* ± 4 kbar, or 30% of the estimated value. This 1s uncertainty represents the entire width of the spinel-peridotite stability field at this *T* (Fig. 10). A better precision of $\pm 5\%$ would give an error of ± 2 kbar, which is more useful, but this precision would have to be maintained down to levels of <100 ppm Ca to be useful.

However, a more severe effect arises from the uncertainties of geothermometry. Any given geothermometer has an uncertainty (combining EMP errors and the uncertainties in the experimental calibration) on the order of $\pm 50^\circ\text{C}$, while the

temperature estimates obtained by the application of different geothermometers to a sample commonly differ by more than 100°C , even in samples screened for homogeneity and equilibrium (Table 2). For an olivine with 600 ppm CaO and a nominal *T* of 1100°C , a variation of 100°C will produce a difference of 17–18 kbar in the pressures obtained by use of the Ca-in-olivine geobarometer. The $\pm 50^\circ\text{C}$ uncertainty expected in an individual geothermometer corresponds to a pressure uncertainty of ± 8 –9 kbar, or more than the entire width of the spinel-lherzolite stability field. Thus the use of the Ca-in-olivine barometer in this *P-T* range does not provide more constraint on pressure than that provided simply by the stability field defined by the presence of the two pyroxene + olivine + spinel mineral assemblage. Given the combined analytical and thermometric uncertainties, it is not surprising that the *PT* points calculated using the Ca-in-olivine barometer for spinel lherzolite xenoliths from Australia and China scatter widely about the relatively well-constrained pyroxenite geotherm in Fig. 10, regardless of the geothermometer applied (Table 2).

Conclusions

(1) Ca in the olivine of 54 spinel peridotite xenoliths from eastern Australia and China ranges from 40–1200 ppm, and is well correlated with Ti, which ranges from <5 to >120 ppm. Neither element is correlated with Fe. This Ca–Ti correlation appears to be dependent on *T*.

(2) Fe and Mn are higher, and Ni lower, in the olivine of Phanerozoic spinel lherzolites than in the olivine of garnet peridotite xenoliths in kimberlites erupted through Archaean terranes. Good correlations exist among these elements irrespective of mineralogy; the differences between the two data sets reflect differences in bulk composition, related to fundamental differences in fertility between Archaean and Phanerozoic subcontinental lithosphere (Boyd, 1996).

(3) Fe and Zn are well correlated in olivine from the garnet peridotite xenoliths, but not in olivine from spinel lherzolites, where Zn contents are lower by ca. 50% than would be predicted by the garnet-peridotite correlation. The difference reflects the strong partitioning of Zn into small amounts of spinel in the shallower rocks.

(4) Ca contents of olivine in spinel peridotites correlate well with temperature as measured by several geothermometers; the slope of the correlation changes above 1000°C, and this may reflect changes in the behaviour of the coexisting clinopyroxene above this *T*.

(5) Pressure estimates for the spinel lherzolites, calculated from the Ca-in-olivine geobarometer (Köhler and Brey, 1990) do not correlate with *T* estimates sufficiently well to be useful in constraining *P-T* conditions within the spinel-lherzolite stability field, especially in regions of a high geotherm.

Acknowledgements

We thank Tin Tin Win for assistance with the analyses, Jingfeng Guo for help with the error analysis, and Sally-Ann Hodgekiss for graphics. Y. Chen prepared some of the Australian samples for proton microprobe analysis. D. Chen's work in Australia was supported by an Australia-Chinese Academy of Science exchange program of the Australian Academy of Sciences, and the research by grants from the Australian Research Council. We thank Gerhard Brey for many discussions on geothermobarometry and Norm Pearson for assistance with geothermobarometry programs. Norm Pearson, Jing Guo, Marc Norman, Michel Gregoire, Ming Zhang, Dmitri Ionov and an anonymous reviewer made helpful comments on the original manuscript. This is contribution no. 78 from the National Key Centre for Geochemical Evolution and Metallogeny of Continents.

References

- Adams, G.E. and Bishop, F.C. (1982) Experimental investigation of Ca-Mg exchange between olivine, orthopyroxene and clinopyroxene: potential for

geobarometry. *Earth Planet. Sci. Lett.*, **57**, 241–50.
Adams, G.E. and Bishop, F.C. (1986) The olivine-clinopyroxene geobarometer: experimental results in the CaO-FeO-MgO-SiO₂ system. *Contrib. Mineral. Petrol.*, **94**, 230–7.

Aoki, K. and Shiba, I. (1973) Pyroxenes for lherzolite inclusions of Itinomegata, Japan. *Lithos*, **6**, 41–51.

Artioli, G., Rinaldi, R., Wilson, C.C. and Zanazzi, P.F. (1995) High temperature Fe-Mg cation partitioning in olivine: in-situ single-crystal neutron activation study. *Amer. Mineral.*, **80**, 197–200.

Boyd, F.R. (1989) Compositional distinction between oceanic and cratonic lithosphere. *Earth Planet. Sci. Lett.*, **96**, 15–26.

Boyd, F.R. (1996) Origins of peridotite xenoliths: major element considerations. In: *High Pressure and High Temperature Research on Lithosphere and Mantle Materials* (G. Ranalli, F. Ricci Lucchi, C.A. Ricci and Trommsdorff, eds), University of Siena Press, Italy, in press.

Brey, G.P. and Köhler, T. (1990). Geothermobarometry in four-phase lherzolites. II. New thermobarometers, and practical assessment of existing thermobarometers. *J. Petrol.*, **31**, 1353–78.

Chen Y.D., Pearson, N.J., O'Reilly, S.Y. and Griffin, W.L. (1991) Applications of olivine-orthopyroxene-spinel oxygen geobarometers to the redox state of the upper mantle. *J. Petrol.*, Special Volume, 291–306.

Dostal, J., Dupuy, C., Zhai, M. and Zhi, X. (1988) Geochemistry and origin of Pliocene alkali basaltic lavas from Anhui -Jiangsu, eastern China. *Geochem. J.*, **22**, 165–76.

Finnerty, A. A. (1989) Inflected mantle geotherms from xenoliths are real: evidence from olivine barometry. In *Kimberlites and Related Rocks* (J. Ross, ed.). Proc. 4th International Kimberlite Conference, Perth, Australia, 1986, Vol.2, *Spec. Publ. Geol. Soc. Aust.*, **14**, Blackwells, pp. 883–900.

Finnerty, A.A. and Boyd, F.R. (1978) Pressure-dependent solubility of calcium in forsterite coexisting with diopside and enstatite. *Carnegie Inst. Wash. Yearbook* **77**, 13–717.

Griffin, W.L. (1987) "On the eclogites of Norway" - 65 years later. *Mineral. Mag.*, **51**, 333–43.

Griffin, W.L., Wass, S.Y. and Hollis, J.D. (1984) Ultramafic xenoliths from Bullenmerri and Gnotuk maars, Victoria, Australia: petrology of a sub-continental crust-mantle transition. *J. Petrol.*, **25**, 53–87.

Griffin, W.L., O'Reilly, S.Y. and Stabel, A. (1988) Mantle metasomatism beneath western Victoria, Australia II: isotopic geochemistry of Cr-diopside lherzolites and Al-augite pyroxenites. *Geochim. Cosmochim. Acta*, **52**, 449–59.

Griffin, W.L., Andi, Z., O'Reilly, S.Y. and Ryan, C.G. (1996) Phanerozoic evolution of the lithosphere beneath the Sino-Korean Craton. In: *Mantle*

- Dynamics and Plate Interactions in East Asia* (M. Flower, S.L. Chung, C.H. Lo and T.Y. Lee, eds) American Geophysical Union Spec. Publ., in press.
- Herzberg, C., (1978) Pyroxene geothermometry and geobarometry: experimental and thermodynamic evaluation of some subsolidus phase relations involving clinopyroxenes in the system CaO-MgO-Al₂O₃-SiO₂. *Geochim. Cosmochim. Acta*, **42**, 945–57.
- Köhler, T.P. and Brey, G. (1990) Calcium exchange between olivine and clinopyroxene calibrated as a geothermobarometer for natural peridotites from 2 to 60 kb with applications. *Geochim. Cosmochim. Acta*, **54**, 2375–99.
- Nixon, P.H. 1987. Kimberlitic xenoliths and their cratonic setting. In: *Mantle Xenoliths* (P.H. Nixon, ed.), J. Wiley and Sons, New York. pp. 215–39.
- O'Neill, H.St.C., (1981) The transition between spinel lherzolite and garnet lherzolite, and its use as a geobarometer. *Contrib. Mineral. Petrol.*, **77**, 185–94.
- O'Neill, H.St. C. and Wall, V.J. (1987) The olivine-orthopyroxene-spinel oxygen geobarometer, the nickel precipitation curve, and the oxygen fugacity of the Earth's upper mantle. *J. Petrol.*, **28**, 1169–91.
- O'Reilly, S.Y. and Griffin, W.L. (1985) A xenolith-derived geotherm for southeastern Australia and its geophysical implications. *Tectonophysics*, **111**, 41–63.
- O'Reilly, S.Y. and Griffin, W.L. (1988) Mantle metasomatism beneath Victoria, Australia I: metasomatic processes in Cr-diopside lherzolites. *Geochim. Cosmochim. Acta*, **52**, 433–47.
- O'Reilly, S.Y. and Griffin, W.L. (1995) Trace element partitioning between garnet and clinopyroxene in mantle-derived pyroxenites: P-T-X controls. *Chem. Geol.*, **121**, 105–30.
- O'Reilly, S.Y., Griffin, W.L. and Ryan, C.G. (1991) Residence of trace elements in metasomatized spinel lherzolite xenoliths: a proton-microprobe study. *Contrib. Mineral. Petrol.*, **109**, 98–113.
- Ryan, C.G., Cousens, D.R., Sie, S.H., Griffin, W.L. and Clayton, E.J. (1990) Quantitative PIXE microanalysis in the geosciences. *Nucl. Instr. and Meth.*, **B47**, 55–71.
- Sachtleben, T. and Seck, H. A. (1981) Chemical control of Al-solubility in orthopyroxene and its implications on pyroxene geothermometry. *Contrib. Mineral. Petrol.* **78**, 157–65.
- Stephenson, P.J. (1989) East Australian volcanic geology of Northern Queensland. In: *Intraplate Volcanism in Eastern Australia and New Zealand* (R.W. Johnson, ed.) Cambridge University Press, 89–97.
- Wass, S.Y. (1973) The origin and petrogenetic significance of hour-glass zoning in titaniferous clinopyroxenes. *Mineral. Mag.*, **39**, 133–44.
- Wass, S.Y. (1979) Multiple origins of clinopyroxenes in alkali basaltic rocks. *Lithos*, **12**, 115–32.
- Wells, P.R.A. (1977) Pyroxene thermometry in simple and complex systems. *Contrib. Mineral. Petrol.*, **62**, 129–39.
- Witt-Eickschen, G. and Seck, H.A. (1991) Solubility of Ca and Al in orthopyroxene from spinel peridotite: an improved version of an empirical geothermometer. *Contrib. Mineral. Petrol.*, **106**, 431–9.
- Xu, X., O'Reilly, S.Y., Zhou, X. and Griffin, W.L. (1996) The Nature of the Cenozoic Lithosphere at Nushan, Eastern China. In: *Mantle Dynamics and Plate Interactions in East Asia* (M. Flower, S.L. Chung, C.H. Lo T.Y. and Lee, eds) American Geophysical Union Spec. Publ., in press.
- Yagi, K. and Onuma, K. (1967) The join CaMgSi₂O₆-CaTiAl₂O₆ and its bearing on the titanaugites. *J. Fac. Sci. Hokkaido Univ. Ser. iv.* **13**, 117–38.

[Manuscript received 22 July 1996;
revised 27 September 1996]